ELSEVIER

Journal of Power Sources 75 (1998) 108–115

JOURNAL OF POWER SOURCES

Performance and life of 10-kW molten-carbonate fuel cell stack using Li/K and Li/Na carbonates as the electrolyte

Yoshihiro Mugikura [a,*], Fumihiko Yoshiba [a], Yoshiyuki Izaki [a], Takao Watanabe [a], Kou Takahashi [b], Sei Takashima [b], Toshiki Kahara [b]

[a] *Central Research Institute of Electric Power Industry, 2-6-1 Nagasaka, Yokosuka-shi, Kanagawa-ken 240-01 Japan*
[b] *Hitachi Works, Hitachi, 3-1-1 Saiwaicho, Hitachi-shi, Ibaraki-ken, 317, Japan*

Received 27 March 1998; accepted 1 May 1998

Abstract

NiO cathode dissolution is a serious problem with molten carbonate fuel cells (MCFC). The target life-time of such cells is 40,000 h, but shorting by NiO cathode dissolution markedly decreases cell performance. NiO cathode dissolution depends on the composition of the molten carbonate electrolyte. The electrolyte generally comprises a mixture of lithium carbonate and potassium carbonate. Since the solubility of NiO in a mixture of lithium carbonate and sodium carbonate is lower than in lithium and potassium carbonate, it is expected that shorting by NiO cathode dissolution will take longer in a mixture of lithium and sodium. Therefore, a mixture of lithium carbonate and sodium carbonate is a strong candidate electrolyte. A unique 10-kW class stack, which uses a mixture of lithium and potassium carbonate and mixture of lithium and sodium carbonate as the electrolyte, has been developed and tested. The basic performance and life time of both electrolyte cells of the stack are reported. In particular, the change in cathode polarization caused by NiO cathode dissolution is evaluated quantitatively.

Keywords: Cell life; Cathode dissolution; Molten carbonate; Fuel cell; Performance

1. Introduction

The molten-carbonate fuel cell (MCFC) is expected to be a more efficient natural gas and coal gas fuelled energy conversion plant than conventional thermal plants. Research and development on MCFCs have been performed in several countries. In Japan, a 1000-kW MCFC pilot plant has been under construction and will be operated from 1999 [1].

Pressurized operation of MCFC is an effective way to improve cell performance; it accelerates the dissolution of the NiO cathode into the matrix. The NiO cathode dissolves as the Ni^{2+} ion [2–12] which is reduced to metallic Ni by H_2 in the fuel gas and bridges the anode and the cathode. Such bridges cause short circuits, degrade cell performance and shorten cell life. Short circuits were observed in tests of a 100-kW stack [13].

State-of-the-art MCFCs generally use a mixture of lithium carbonate and potassium carbonate (Li/K) as the electrolyte. A cell which uses a mixture of lithium carbonate and sodium carbonate (Li/Na) would have a longer life-time since solubility of NiO in Li/Na is lower than that in Li/K. In addition, the ionic conductivity of Li/Na is higher than that of Li/K [14,15], but oxygen solubility in Li/Na is lower than in Li/K. Although several Li/Na single cells have been tested and their basic characteristics reported [14,15], the performance and lifetime of Li/Na stacks are not known. A unique 10-kW class MCFC stack which uses Li/K and Li/Na electrolytes has been developed and tested, since the performance and life-time of each electrolyte have to be evaluated under the same conditions. The basic performance and cell life-times of the Li/K cells and Li/Na cells of the stack have been examined. In addition, the change in cathode polarization caused by NiO dissolution has been elucidated by a new performance analysis method. Such detailed analysis of the degradation in stack performance with time has not been

* Corresponding author. Tel.: +81-468-56-21-21; Fax: +81-468-57-30-72

0378-7753/98/$19.00
PII S0378-7753(98)00103-7

previously reported. After operation, the stack has been analyzed to determine the change in performance with time.

2. Experimental

The stack consisted of 26 cells. The cell area was 2520 cm^2. The electrolyte of six cells, which were located at top of the stack, was $(Li/Na)CO_3$ ($Li/Na = 53/47$ mol%). The other cells used $(Li/K)CO_3$ ($Li/K = 62/38$ mol%). The anode was made of Ni–Al alloy. The cathode was NiO. The stack employed light separator plates which were newly developed. The new separator plate consisted of thin stainless-steel plates. The gas flow pattern of the stack was the cross-flow type. Cell components, such as the anode, the cathode and the separator plate, of the Li/K and Li/Na cells were the same. Differences in the performance and life-time were therefore attributed to the electrolyte composition.

The stack was established at the test facility of CRIEPI after an initial check of performance of the stack with heating up and cooling down processes at the Hitachi Works site. The stack was operated over the pressure range of 3 to 7 ata. No gas recycling, such as cathode gas recycling, was applied. The flow rate of the cathode gas was changed to control the stack temperature. The temperature of the cathode inlet gas was fixed at 580°C. The temperature of the anode inlet gas was fixed at 600°C to prevent carbon deposition from the anode gas. The maximum temperature in the stack was kept below 680°C. The current density was controlled by an electric load.

Effects of pressure, current density, fuel utilization and oxidant gas composition on stack performance were measured before 1000 h. Continuous operation at a constant condition was begun after 1000 h. In the continuous operation, the cathode CO_2 partial pressure was 1.4 ata and was chosen to accelerate NiO cathode dissolution. The final operation time was 5700 h. During the operation, the effects of pressure and oxidant gas composition on the stack performance were measured at intervals. A current-interrupter method (a non-steady-state) measurement was applied to obtain the open-circuit voltage (OCV) and the response of voltage recovery. After operation, tests to determine the amount of nickel in the matrix and the corrosion depth were performed.

3. Results and discussion

The voltage–current characteristic of the stack at 7 ata is shown in Fig. 1. The maximum current density was 187.5 mA cm^{-2} and the maximum power density was 1.4 kW m^{-2}, which was calculated using the overall mean cell

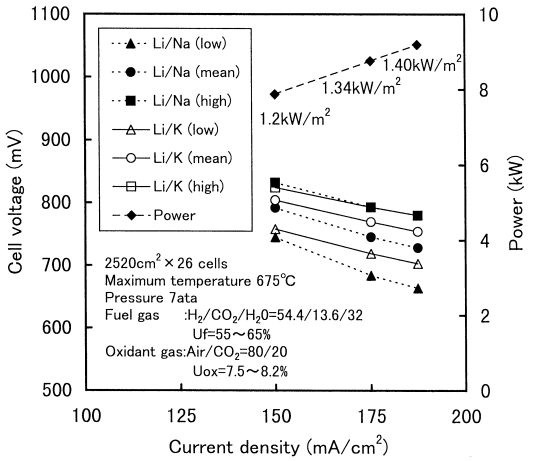

Fig. 1. Voltage–current characteristics of a 10-kW MCFC stack.

voltage. The maximum temperature in the stack at 187.5 mA cm^{-2} became higher than 680°C since the flow rate of the cathode gas (which was used to cool down the stack) was insufficient.

The mean voltage of the Li/K cell was higher than that of the Li/Na cell in the measured pressure range. The cell components of the Li/Na cell were the same as those of the Li/K cell and were not optimized. The Li/Na cell, which uses optimized cell components, would have better performance since the maximum cell voltage was equal to that of the Li/K cell. The Li/Na cell performance depends strongly on temperature compared with that of the Li/K cell [14,15]. The cell (No. 1) with the poor performance was located at the top of the stack. Its temperature was the lowest among the cells, as shown in Fig. 8. This was the cause of its inferior performance. The difference between the high cell voltages of Li/K and Li/Na was expected to decrease at current densities higher than 150 mA cm^{-2}, since the ionic conductivity of Li/Na is lower than that of Li/K. The difference did not decrease, however, since the temperature of the Li/Na cell became low

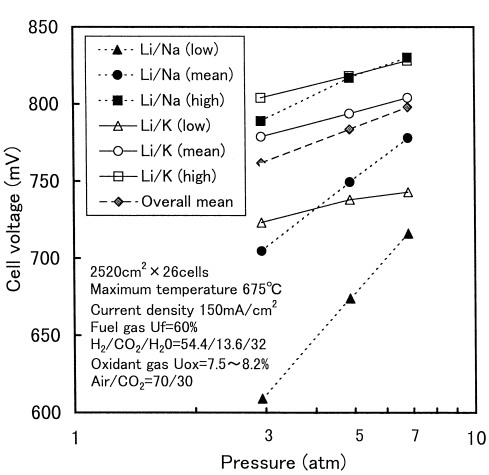

Fig. 2. Effect of pressure on cell performance in the stack.

because of high cathode flow rate used to cool the stack at higher current densities.

The effect of pressure on cell voltage is shown in Fig. 2. The maximum cell voltage of the Li/Na cell was lower than that of the Li/K cell at 3 ata. Nevertheless, the pressure gain of the Li/Na cell was approximately 120 mV/decade and was twice that of the Li/K cell. The gain agreed with the result found for a small single cell [14,15]. The maximum cell voltage of the Li/Na cell was higher than that of the Li/K cell at pressures higher than 5 ata. Thus, the Li/Na cell has the advantage of high performance in the pressurized operation.

The performance of each cell in the stack was analyzed by the special method [16–18]. The cathode reaction resistance (R_c) of a single cell obeys the following equation:

$$R_c = AP_{O_2}^{-0.75}P_{CO_2}^{0.5} + BP_{CO_2}^{-1} \quad (1)$$

This equation was derived from consideration of the diffusion processes of super-oxide ion and CO_2 in the electrolyte [19]. The output voltage (V) of each cell in the stack can be expressed by Eq. (2) using the OCV (E), the Nernst loss (η_{NE}), the anode reaction resistance (R_a), the cathode reaction resistance, and the internal resistance (R_{ir}) if the anode and the cathode polarization are both proportional to current density (J):

$$V = E - \eta_{NE} - J(R_a + R_c + R_{ir}) \quad (2)$$

E and η_{NE} were calculated using a single cell performance model [20]. R_{ir} observed at approximately 600°C was compensated using the representative temperature of the stack. The temperature of the stack was not uniform. In the analysis, 650°C was assumed as the representative stack temperature. R_a is almost constant and smaller than R_c if the fuel gas is reformed LNG [19–21].

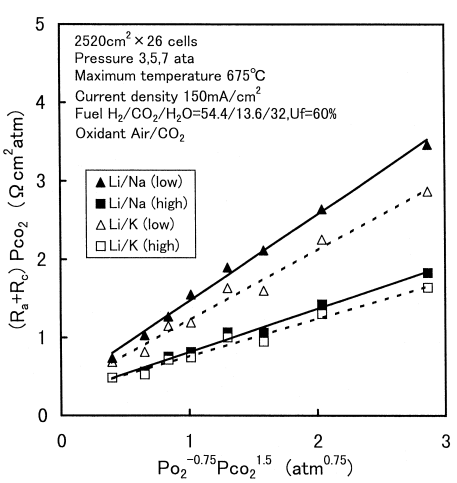

Fig. 3. Relationship based on Eq. (3).

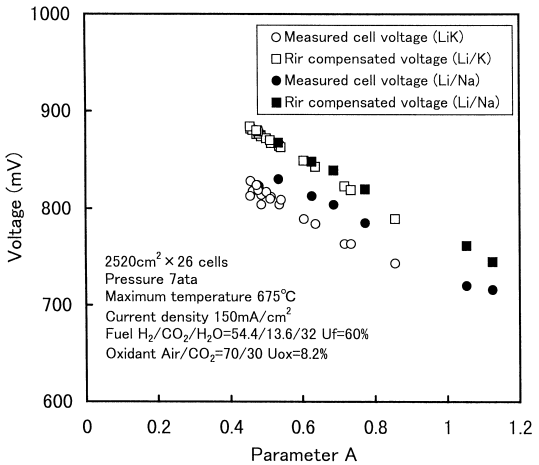

Fig. 4. Relationship between cell voltage and parameter A in Eq. (1).

To confirm the effect of cathode gas composition on cathode reaction resistance, Eq. (1) was arranged and the following equation was obtained:

$$(R_c + R_a)P_{CO_2} = AP_{O_2}^{-0.75}P_{CO_2}^{1.5} + B + R_aP_{CO_2} \quad (3)$$

The $R_a + R_c$ for each cell was calculated from observed stack performance based on Eq. (2). Plots based on Eq. (3) display good linear relationships, see Fig. 3. It was confirmed that the cathode reaction resistance of the stack obeyed Eq. (1), as found for single cells. Parameters A and B in Eq. (1) and R_a were determined from the dependence of the cathode reaction resistance on the cathode gas composition. The relationship between cell voltage and parameter A is presented in Fig. 4. The cell voltage compensated by R_{ir} is proportional to parameter A. This suggests that the diffusion of super-oxide ion in the electrolyte plays an important role in the cathode reaction.

The voltage drops caused by the internal resistance, the anode polarization and the cathode polarization were calculated using parameters A, B and R_a. The performance of each cell at 540 h is given in Fig. 5. The anode and cathode voltage drops analyzed by this method agree with the results obtained from single cell tests. The method is able to analyze the performance of each cell in the stack with good accuracy. The voltage drop caused by the internal resistance in all Li/Na cells (Nos. 1–6) is almost half of that of Li/K cells (Nos. 7–26) since the ionic conductivity of Li/Na is approximately twice that of Li/K. The cathode voltage drop of the top (No. 1) and bottom (No. 26) cells in the stack is large since the temperatures of these cells are lower than those of the middle cells, as shown in Fig. 8. In addition, the cathode voltage drop in all the Li/Na cells is larger than that of the Li/K cells since the temperature dependence of R_c of the Li/Na cells is larger than that of the Li/K cells [15]. There is a temperature region lower than 620°C in the stack. Temperature control of the stack is very important, particularly in the case of a Li/Na stack.

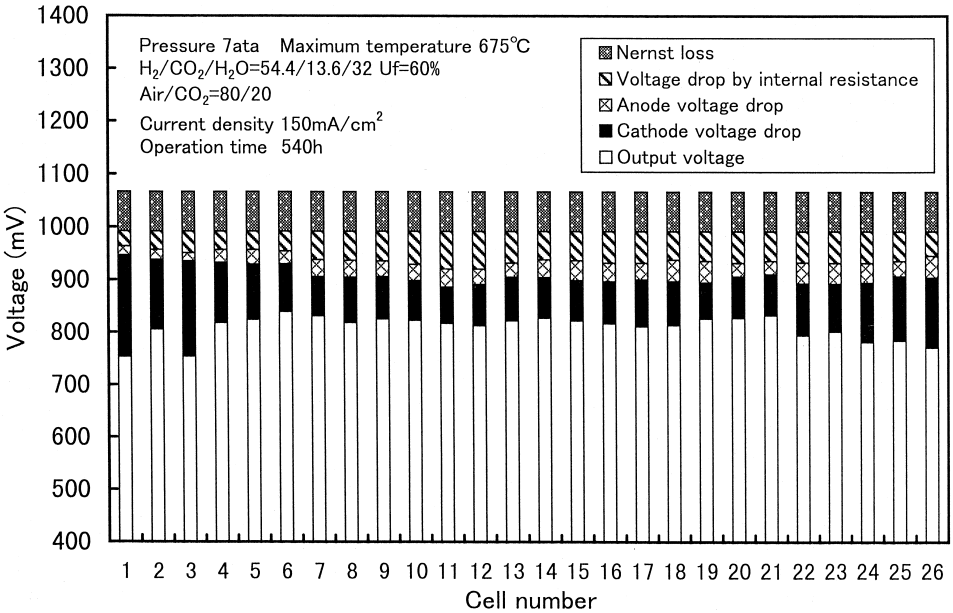

Fig. 5. Analysis of the performance of each cell in a 10-kW MCFC stack at 540 h.

The history of stack performance is presented in Fig. 6. The stack has been basically operated under constant conditions after the initial stack performance was determined. The operating pressure was fixed at 7 ata during continuous operation. The cathode gas composition was: air/CO_2 = 80/20. The cathode CO_2 partial pressure was 1.4 ata and was chosen to accelerate NiO cathode dissolution. Both Li/K and Li/Na cells exhibited stable performance until 1400 h. The mean cell voltage of Li/K cells, however, began to drop after 1400 h. This is assumed to be due to shorting by NiO cathode dissolution. The anode inlet and outlet gas compositions were analyzed by gas chromatography in parallel with the operation. The fuel consumption by the cell reaction, combustion and methanation were calculated from the mass balance between the anode inlet and outlet gas compositions. The shorting current density was calculated from the difference between the set fuel utilization and the calculated fuel utilization from the mass balance. The history of the shorting current density is also shown in Fig. 6. This began to increase gradually at approximately 1400 h, in agreement with the behaviour of the mean cell voltage of Li/K cells. As a result, the voltage drop of the Li/K cell after 1400 h is caused by shorting.

An empirical equation for the shorting time has been proposed [7] from several single tests, viz.,

$$t_{SC} = 7.22 \times 10^4 \ell^{1.67} P_{CO_2}^{-0.93} \quad (4)$$

where: t_{SC} is the shorting time (h); ℓ is the matrix thickness (cm); P_{CO_2} is the cathode CO_2 partial pressure (atm).

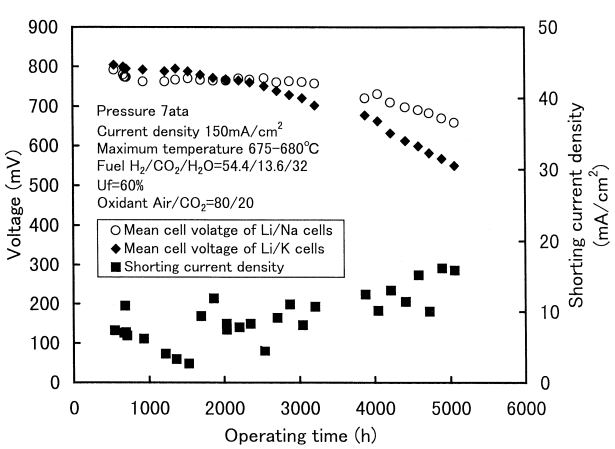

Fig. 6. Performance of a 10-kW MCFC stack.

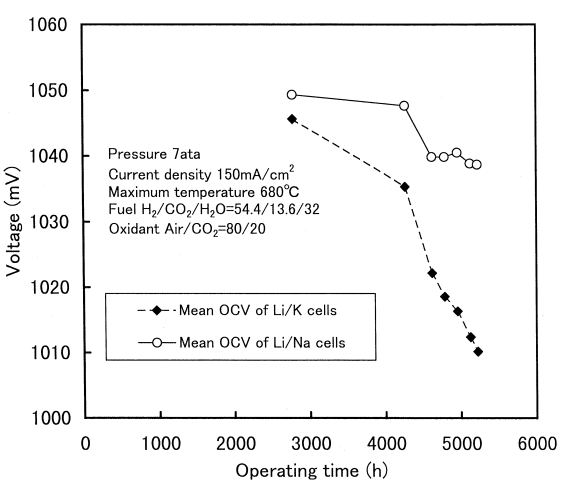

Fig. 7. Open-circuit voltage of a 10-kW MCFC stack determined by a current interrupter method.

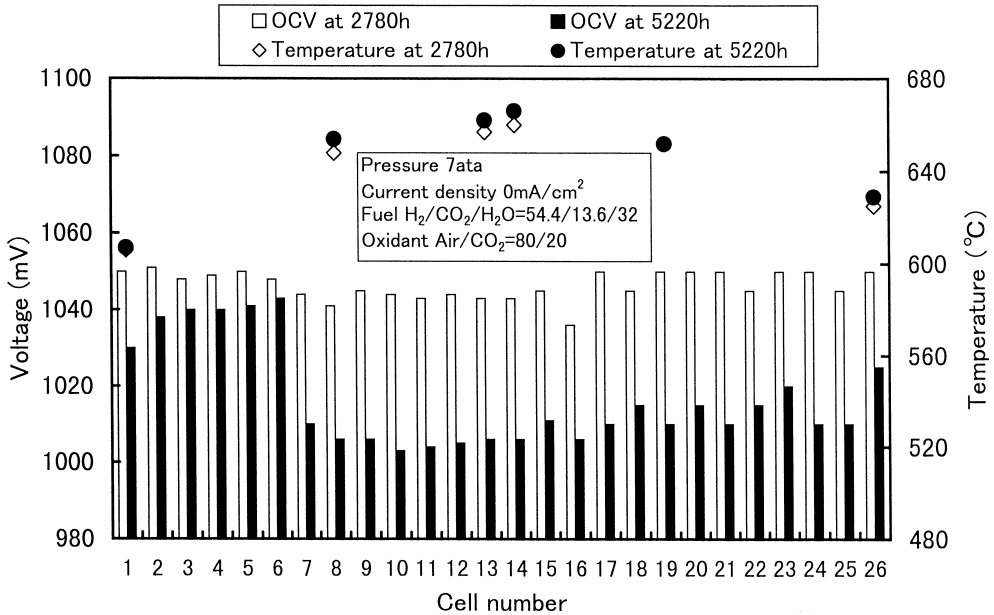

Fig. 8. Cell temperature and open-circuit voltage of a 10-kW MCFC stack.

The shorting time calculated by Eq. (4) was 1358 h and the measured shorting time was 1400 h. These times are in a good agreement in spite of the fact that the stack used cell components which were different from those employed in single cells to derive Eq. (4). The mean cell voltage of Li/Na cells also began to drop after 3000 h. The shorting by NiO dissolution is assumed to be a cause of the fall in voltage, since no external short circuit around the stack was observed after operation. The Ni deposition rate and the amount of Ni in the matrix are important factors [8] in the shorting phenomena. The amount of Ni in both matrixes at the shorting time will be the same since specifications of matrixes of Li/K and Li/Na cells are the same. The Ni deposition rate of the Li/K cell will be twice as fast as that of the Li/Na cell. The OCVs of Li/K cells and Li/Na cells were measured by a current interrupter method. The relaxation in voltage after immediate current shut down was observed by means of a digital oscilloscope. No change in the stack temperature was observed during the measurement. The measured OCVs

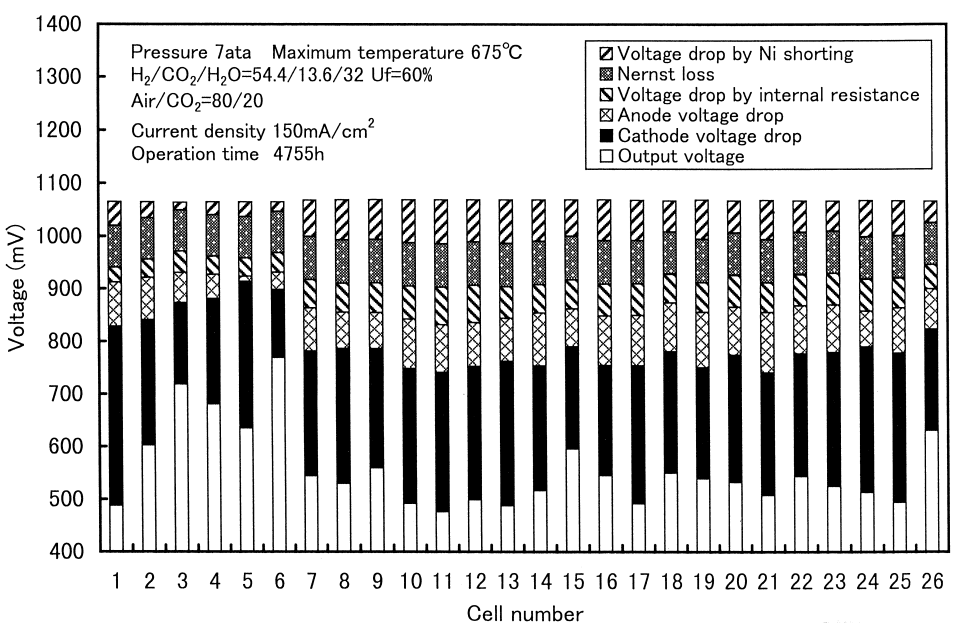

Fig. 9. Analysis of the performance of each cell in a 10-kW MCFC stack at 4755 h.

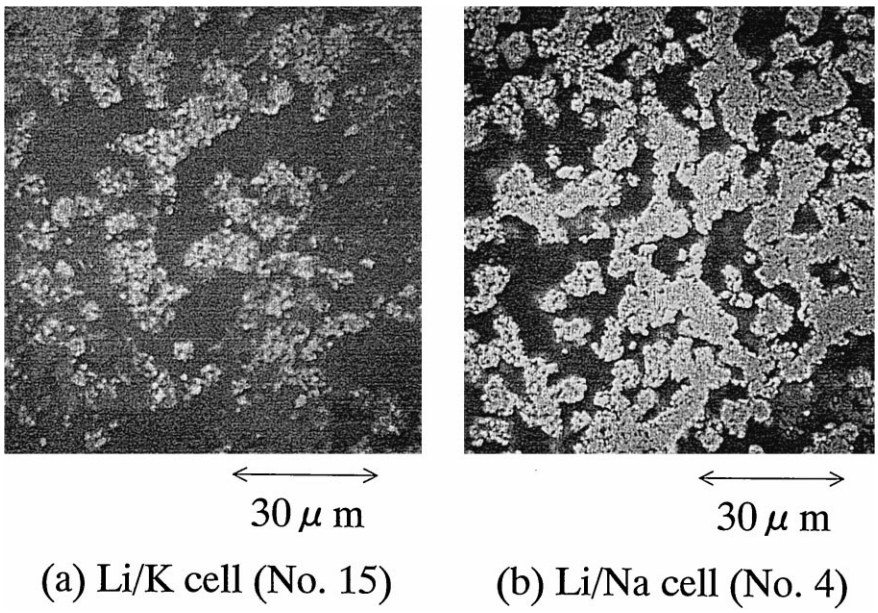

Fig. 10. Structures of cathodes after operation.

are shown in Fig. 7. The mean OCV of Li/K cells was considerably lower than that of Li/Na cells at 5000 h. The shorting currents of Li/K cells are greater than those of Li/Na cells. The mean OCV of Li/K cells decreases with operation time. The falls in the OCVs of Li/K and Li/Na cells are caused by shorting.

The profiles of cell temperature and OCV of the stack are shown in Fig. 8. The temperature profiles at 2780 and 5220 h are almost same since the stack temperature was controlled by increase in the cathode gas flow rate. The difference in OCVs increased, however, with operating time. All the OCVs of Li/K and Li/Na cells at 2780 h were almost same. By contrast, the OCVs of Li/K cells (Nos. 7–26) are obviously lower than those of Li/Na cells (Nos. 1–6) at 5220 h. Considerable current was exhausted by the shorting.

Each cell performance at 4755 h was analyzed from the dependence of the cathode reaction resistance on the gas composition. The shorting current was estimated by using the OCV determined by a current interrupter method; the results are presented in Fig. 9. It was not possible to measure the internal resistance of each cell. The change of internal resistance with time was included in the change of anode voltage loss since the internal resistance was assumed to be the same during the operation. The voltage drop caused by the shorting includes the Nernst loss, the anode voltage drop and the cathode voltage drop. From a comparison of the data in Figs. 5 and 9, the shorting and the cathode voltage drop are the major determinants of cell performance degradation with time. The cathode voltage drop was larger than the voltage drop by the shorting. The former is caused by the cathode structure change and electrolyte loss. The NiO cathode is dissolved into the matrix and changes the structure. Electrolyte was consumed by the corrosion of the current collector and creepage. Cathode polarization is a function of the electrolyte fill level of the cathode. This level is set at an optimum value in the cell design. The change in cathode structure

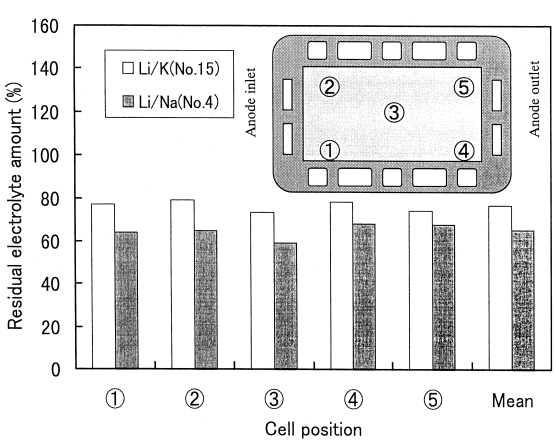

Fig. 11. Residual electrolyte amount after operation.

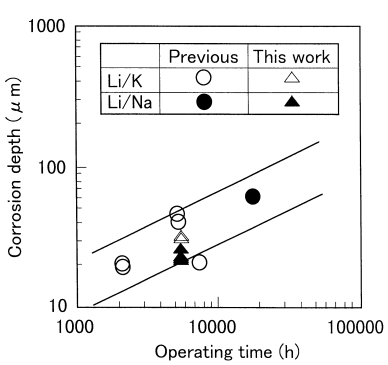

Fig. 12. Corrosion depths of cathode current-collectors.

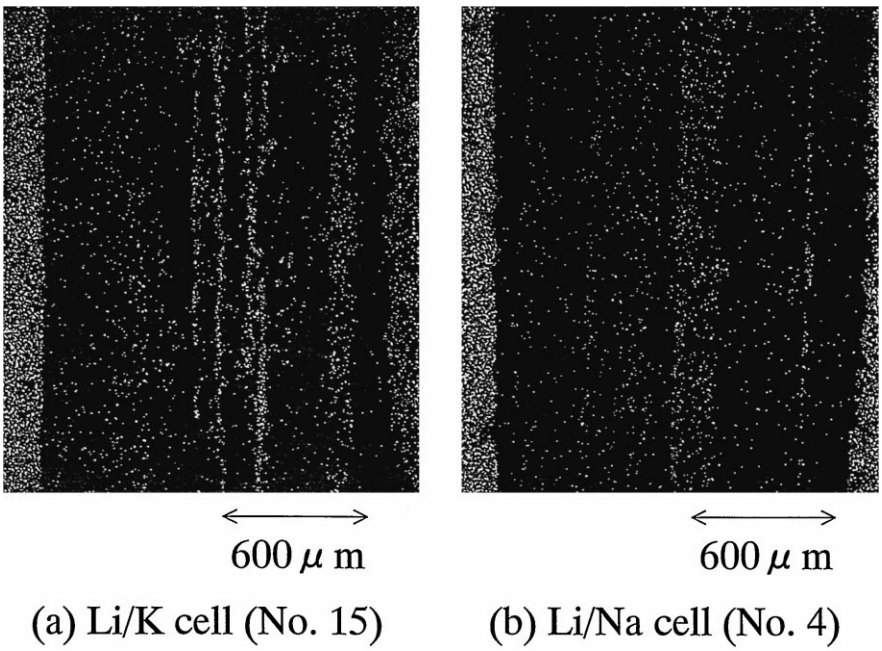

Fig. 13. Nickel maps of matrix cross-sections.

and the electrolyte loss change the electrolyte fill level of the cathode.

After the operation, the structures of the cathodes of the Li/K and Li/Na cells were analyzed. Electron micrographs are shown in Fig. 10a and b. The structure of the operated Li/K cell is different from the initial structure. The pore size of the Li/K cell becomes larger than that of the Li/Na cell despite the fact that these cells used the same electrodes. The amount of residual electrolyte in both cells was determined, as shown in Fig. 11. The Li/K cell lost approximately 20% of the electrolyte while the Li/Na cell lost 30%. Severe corrosion was anticipated in the Li/Na cell. The depth of corrosion of the cathode current-collectors of both cells was measured, see Fig. 12. No difference is observed in the corrosion depth of Li/K and Li/Na cells. No significant corrosion of the current-collector occurred in the Li/Na cell. This suggests that the reason for the difference in the electrolyte loss of Li/K and Li/Na cells is not corrosion but the creepage of Li/Na electrolyte.

The cell performance depends strongly on amount of the electrolyte in the cathode. The distribution of electrolyte in a MCFC is controlled by capillary forces since MCFCs use porous components. All pores of the matrix are filled with electrolyte because this component has the smallest pore size. The electrolyte fill levels of the electrodes depend on the pore sizes of the anode and the cathode. The control of the pore sizes is an important technology. The capillary force in a large pore is weaker than that of a small pore. After operation, the cathode pore size of the Li/K cell becomes considerably larger than that present initially. Thus, the capillary force in the cathode is small. In Fig. 9, the cathode voltage drop of Li/Na is not small even though the change in its structure is not significant. If the cathode voltage drop depends only on the cathode structure, then the performance of only the Li/K cell should be affected. The electrolyte loss in the Li/Na cell, as shown in Fig. 11, affects the cathode voltage drop. The increase in the cathode voltage drop with time is caused by the change in structure and the electrolyte loss. As a result, NiO cathode dissolution causes not only shorting but increases the cathode reaction resistance. This effect has to be considered in the design of a long-life cell.

The matrixes of the Li/K and Li/Na cells were also analyzed; electron micrographs are shown in Fig. 13a and b, respectively. The white dots in the micrographs are deposited Ni particles. The number of Ni particles in the Li/K matrix is obviously larger than in Li/Na matrix.

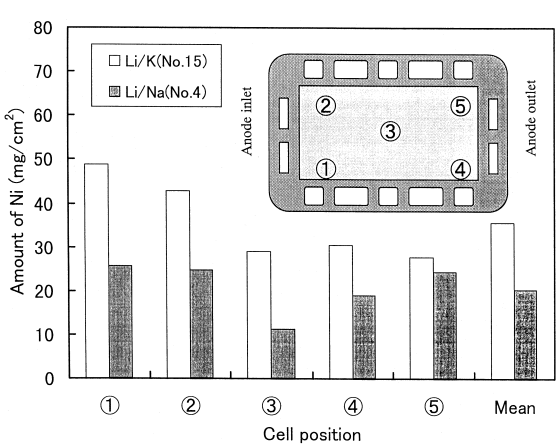

Fig. 14. Amount of nickel in the matrix.

This result agrees with the analyzed amount of Ni in the matrix. The amounts of Ni in the Li/K and Li/Na matrixes are given in Fig. 14. The amount of Ni in the Li/Na cell is approximately half that of the Li/K cell. The difference in the shorting times of Li/K and Li/Na cells is caused by the difference in the Ni deposition rates in Li/K and Li/Na electrolytes. In addition, considerable NiO dissolution in the Li/K cell changes the cathode structure.

4. Conclusions

A 10-kW stack using Li/K and Li/Na electrolytes has been tested for 5700 h at 7 ata. The cathode CO_2 partial pressure was 1.4 ata and was chosen to accelerate NiO cathode dissolution. It is concluded that the life of the Li/Na cell is longer than that of the Li/K cell which is limited by NiO cathode dissolution.

The pressure gain of the Li/Na cell voltage is larger than that of the Li/K cell voltage and is approximately twice that of the Li/K cell voltage. Nevertheless, the Li/Na cell performance depends strongly on temperature. Thus, in operation of the Li/Na stack, temperature control is very important.

The performance of each cell in the stack has been analyzed by an analysis method which uses the dependence of cathode performance on the cathode gas composition. It is confirmed that diffusion of super-oxide ion in the electrolyte plays an important role in cathode polarization.

Shorting by NiO cathode dissolution takes place in Li/K cells at 1400 h. The shorting time agrees with the value estimated from an empirical relationship. In Li/Na cells, the shorting begins at approximately 3000 h. The shorting time of the Li/Na cell is twice that of the Li/K cell. The measured amount of Ni in the Li/K matrix is approximately twice that in the Li/Na matrix. The Ni deposition rate influences the shorting times of Li/K cell and Li/Na cell.

Change in performance of the stack with time was analyzed. The shorting and the cathode voltage drop caused by the change in cathode structure and electrolyte loss are the major factors in cell performance degradation with time.

Measurements were made of the corrosion depths of the cathode current-collectors in both cells. No difference in corrosion depth is observed between Li/K and Li/Na cells. After operation, analysis was made of the structures of the cathodes of Li/K and Li/Na cells. The structure of the Li/K cell changes from the initial structure. The pore size of the Li/K cell becomes larger than that of the Li/Na cell despite the fact that these cells used the same electrodes. The cathode pore size of the Li/K cell becomes considerably larger than the initial size. Considerable electrolyte in the cathode was lost by the structure change and electrolyte loss itself. This increases the cathode reaction resistance.

As a result, the Li/Na cell has the advantage of high performance in pressurized operation. In addition, NiO cathode dissolution causes not only shorting but also increases the cathode polarization. The change in the cathode structure by NiO dissolution is a serious problem and has to be considered in the electrode design.

References

[1] M. OOue, H. Yasue, Fuel Cell Seminar Program and Abstracts, 1996, p. 51.
[2] C.E. Baumgartner, R.H. Arendt, C.D. Ivacovangelo, B.R. Karas, J. Electrochem. Soc. 131 (1984) 2217.
[3] H.R. Kunz, J.W. Pandolfo, J. Electrochem. Soc. 139 (1992) 1549.
[4] D.A. Shore, J.R. Selman, S. Irani, E.T. Ong, Proceedings of the Second Symposium on Molten Carbonate Fuel Cell Technology, 1992, pp. 290–317.
[5] E.T. Ong, Proceedings of The International Fuel Cell Conference, 1992, p. 219.
[6] R.C. Makkus, Electrochemical studies on the oxygen reduction and NiO(Li) dissolution in molten carbonate fuel cell, Pasmans offsetdrukkerij BV, 's-Gravenhage (1991) 55.
[7] Y. Mugikura, T. Abe, S. Yoshioka, H. Urushibata, J. Electrochem. Soc. 142 (1995) 2971.
[8] Y. Mugikura, M. Yoshikawa, Y. Izaki, T. Watanabe, The Second International Fuel Cell Conference Proceedings, 1996, p. 169.
[9] S. Yoshioka, H. Urushibata, J. Electrochem. Soc. 144 (1997) 815.
[10] S. Yoshioka, H. Urushibata, Denki Kagaku 64 (1996) 1074.
[11] J.D. Doyon, T. Gilbert, G. Davies, J. Electrochem. Soc. 134 (1987) 3035.
[12] K. Ota, T. Shinsho, N. Kamiya, Denki Kagaku 55 (1987) 323.
[13] T. Watanabe, T. Abe, Y. Izaki, Y. Mugikura, E. Koda, Fuel Cell Seminar and Abstracts, 1994, p. 446.
[14] S. Yoshioka, H. Urushibata, Denki Kagaku 64 (1996) 909.
[15] M. Yoshikawa, F. Yoshiba, H. Morita, T. Abe, M. Yamaguchi, K. Iwamoto, The Second FCDIC Fuel Cell Symposium Proceedings, 1995, p. 289.
[16] Y. Mugikura, F. Yoshiba, Y. Izaki, T. Watanabe, K. Takahashi, S. Takashima, T. Kahara, 1996 Fuel Cell Seminar Program and Abstracts, 1996, p. 394.
[17] Y. Mugikura, H. Morita, Y. Izaki, T. Watanabe, The 37th Battery Symposium in Japan, 1996, p. 273.
[18] H. Morita, Y. Mugikura, Y. Izaki, T. Watanabe, T. Abe, Denki Kagaku 63 (1995) 1053.
[19] Y. Mugikura, T. Abe, T. Watanabe, Y. Izaki, Denki Kagaku 60 (1992) 124.
[20] Y. Mugikura, H. Morita, Y. Izaki, T. Watanabe, The 4th FCDIC Fuel Cell Symposium Proceedings, May 15–16, Tokyo, 1997, p. 301.
[21] Y. Mugikura, H. Morita, Y. Izaki, T. Watanabe, The Transactions of the Institute of Electrical Engineers of Japan, in press.